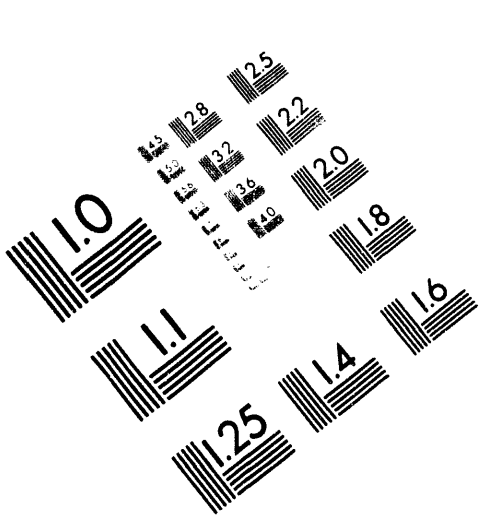

AIIM

Association for Information and Image Management
1100 Wayne Avenue, Suite 1100
Silver Spring, Maryland 20910
301/587-8202

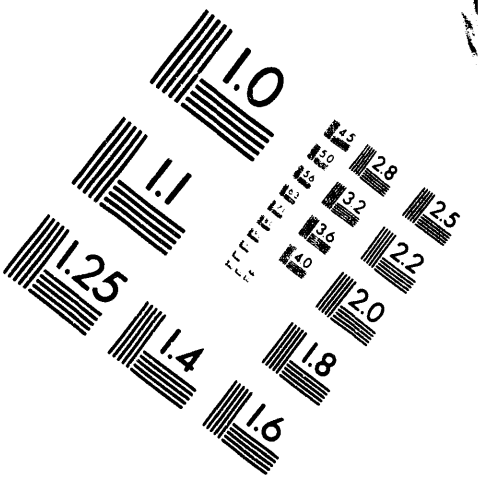

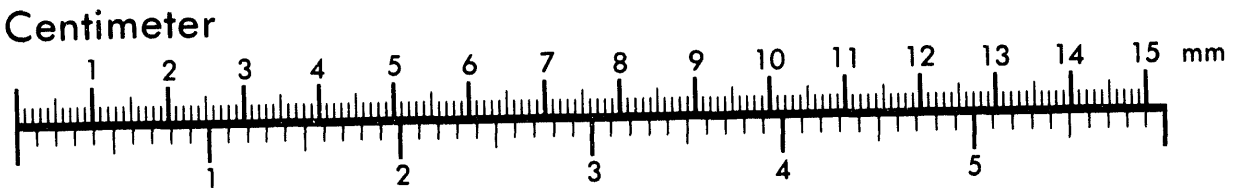

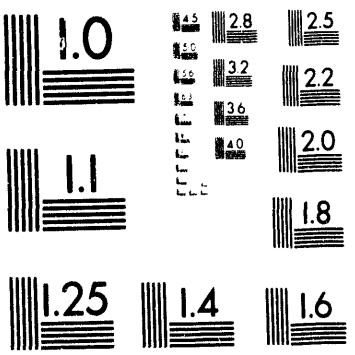

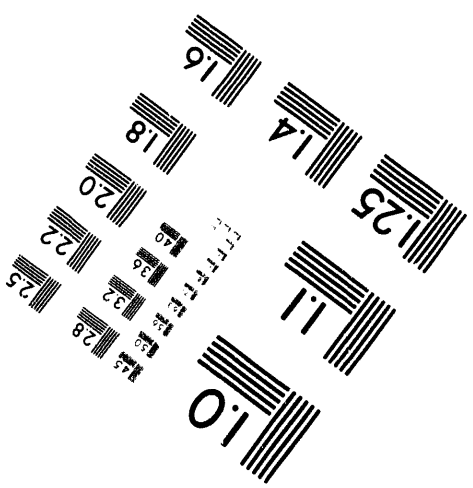

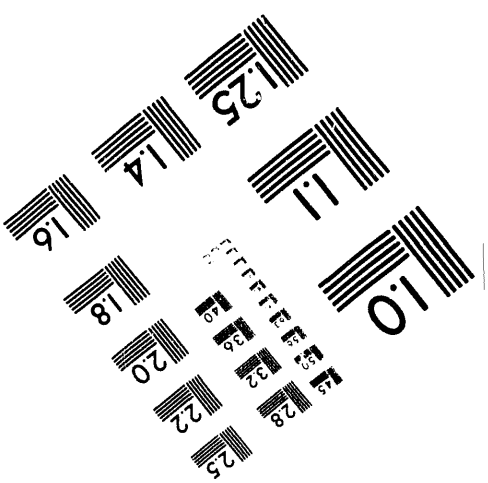

1 of 1

Conf-930616--14

2

ENERGY LOSSES IN SWITCHES*

T. H. Martin, J. F. Seamen, D. O. Jobe†
Sandia National Laboratories
P. O. Box 5800, Albuquerque, NM 87185-5800

DISCLAIMER

Abstract

Our experiments show energy losses between 2 and 10 times that of the resistive time predictions. The experiments used hydrogen, helium, air, nitrogen, SF_6, polyethylene, and water for the switching dielectric. Previously underestimated switch losses have caused overpredicting the accelerator outputs. Accurate estimation of these losses is now necessary for new high-efficiency pulsed power devices where the switching losses constitute the major portion of the total energy loss.

We found that the switch energy losses scale as $(V_{peak}\, I_{peak})^{1.1846}$. When using this scaling, the energy losses in any of the tested dielectrics are almost the same. This relationship is valid for several orders of magnitude and suggested a theoretical basis for these results. Currents up to .65 MA, with voltages to 3 MV were applied to various gaps during these experiments. Our data and the developed theory indicate that the switch power loss continues for a much longer time than the resistive time, τ_r, with peak power loss generally occurring at peak current in a ringing discharge instead of the early current time.

A theory will explain the experimental data. The scaling of the experimental results leads to a spark channel theory developed by Braginiskii[1] for gasses. In his theory, as with τ_r, the spark channel plasma has constant conductivity and the changing spark channel radius causes the channel resistance to decrease as a function of time. The channel balances the I^2 R input power with the shock front, the ionization of new particles, and heating these particles to several ev of temperature. Remarkably, the shock front boundary traps the radiation and little power gets outside the channel.

All of our experiments were circuit code modeled after developing a new switch loss version based on the theory. The circuit code predicts switch energy loss and peak currents as a function of time. During analysis of the data we noticed slight constant offsets between the theory and data that depended on the dielectric. We modified the plasma conductivity for each tested dielectric to lessen this offset.

The calculations gave excellent agreement between theory and experiment. In addition, the new model successfully predicted the series resistance of Marx generators.

Review of the τ_r Method to Calculate Switch Losses

The τ_r method predicts a time, τ_r, for a switch resistance to pass through a matched load condition while going toward a zero value.[2] τ_r is the approximate duration where the switch breakdown impedance matches the driving source impedance. The total source impedance the switch sees consists of both the source and load impedance. Thus the energy delivered to the switch is given by

$$E_{switch} = \frac{1}{4} V_{peak}\ I_{peak}\ \tau_r \qquad (1)$$

V_{peak} and I_{peak} are the open circuit voltage and the short circuit current, as viewed by the switch. The factor of 4 provides the matched load power at the switch. Experiments show that for gas, τ_r is

$$\tau_r = \frac{88 \sqrt{\frac{\rho}{\rho_o}}}{Z^{1/3}\, E^{4/3}} \qquad (2)$$

Z is in ohms; E in 10's of kV per cm; and τ_r is in ns. An alternative for liquids of unit density is given as

$$\tau_r = \frac{5}{Z^{1/3} E^{4/3}} \qquad (3)$$

E is now in MV per cm. The two equations are the same when using water and air densities in equations 2 and 3.

The spark channel is uniform in temperature (constant conductivity) and thus could only allow resistance changes by increasing the spark channel diameter. Measuring the exponential drop of voltage from 100, 10, and 1 ohm transmission lines discharging through switches provided τ_r. The AWE noted only a 10% deviation from an exponential voltage decay. The note presented no raw data.

The accepted method predicts lower loss in gasses than in liquids and in all cases the main power delivered to the channel was during τ_r. In addition, a different energy dissipation mechanism explained energy losses on long time scales, for instance the energy losses used in hydroforming.

The Experiment

The Test Bed

Figure 1 shows the Ripple test-bed circuit diagram. Physics International furnished the low inductance Marx generator for Ripple. The Marx stores a maximum energy of 40 kJ for an output voltage of 3 MV. Thirty-five bipolar capacitors with each capacitor charged to ±50 kV. Total Marx inductance is 3.2 μh. A constant resistance made of wire wound resistors in each stage provide a safety damping resistance of 4.9 ohms. The Marx energy rings forward into a water insulated energy storage capacitor (Intermediate Store) with an end plate. The three transmission lines forming the Intermediate Store (IS) have a total capacity of 8.7 nf. When the test switch breaks the IS discharges into a precisely known inductance (determined from the ringing frequency) which provides a nominal 100 ns to peak current or 200 ns for 1/2 cycle of current. The water stray capacity, nominally .5 nf, provides some interesting effects. V_{SW} measures the switch and inductor voltage and the Current Viewing Resistor (Cvrl) measures the current through the inductor. The relative positions of these two monitors in the water tank require that the data sets be time shifted. We next multiply the two data sets and integrate to provide the forward going energy into the switch and the inductive load. We subtract the inductive load energy of $1/2\, L\, I^2$ and obtain the energy deposited in the switch. In addition, there is the energy deposited in the switch from the stray capacity ($1/2\, C\, V^2$). Normally, but not always, the stray capacity energy is small compared to the total switch energy.

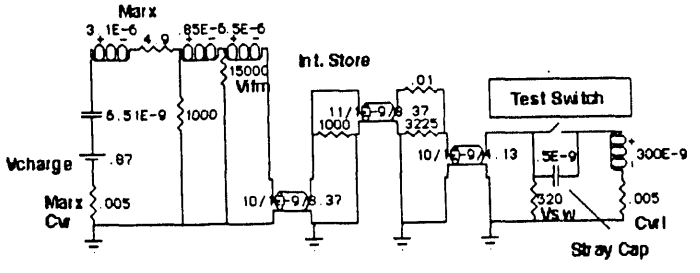

Figure 1

In principle this procedure provides an accurate switch dissipation energy. In practice there are two problems that can give inaccurate results. First, the voltage monitor must accurately respond to the decaying switch voltage. We improved the response by using a low impedance voltage monitor and by improving the frequency response of subsequent attenuator chains. Second, the time shift between the current and voltage monitors must be accurate. Since the monitors are 40 cm apart, the propagation delay in water is about 9 ns. The current monitor worked well. A low-inductance, .005-ohm, fast-response T&M current-viewing resistor gave accurate current readings after we applied a waterproof coating.

A preset Macro program automatically time-shifted, multiplied, integrated and subtracted the current and voltage data sets. The program provides the dissipated energy of the switch as a function of time.

The Calibration Verification

We increased the experiment's credibility by performing the calibration experiment. Unexpectedly, we found how gas switches dissipate their energy and that the type of gas can make a difference in this process.

Providing a calibration over the entire operating range of our experiments is not possible but providing a known energy dissipation in the middle of our data range is feasible. A possible way of doing this might be measuring the energy deposited in the gas by monitoring the pressure change of the gas after a shot.[3] By knowing the type of gas and specific heat then the energy deposited in the gas is easily calculated. The expected energy deposited in our nominal one-liter gap is shown as Fig 2. The actual energy deposited in the gap was compared to the experimental energy obtained with V and I measurements as shown in Fig 3. With the diatomic gases only 40% of the energy is being measured by the change in gas pressure. The monatomic or noble gases did a little better by indicating a 60% deposition but still did not provide the expected result. After comparing the two different gas types and knowing that the theory predicted most of the spark energy was in ionization energy, we reasoned that as the spark channel decayed, its energy was delivered to the spark gap walls and electrodes before the entire volume of gas in the switch was heated.

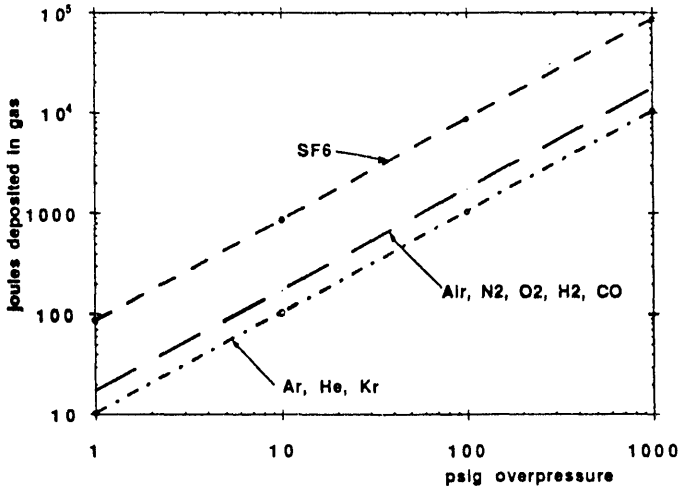

Figure 2

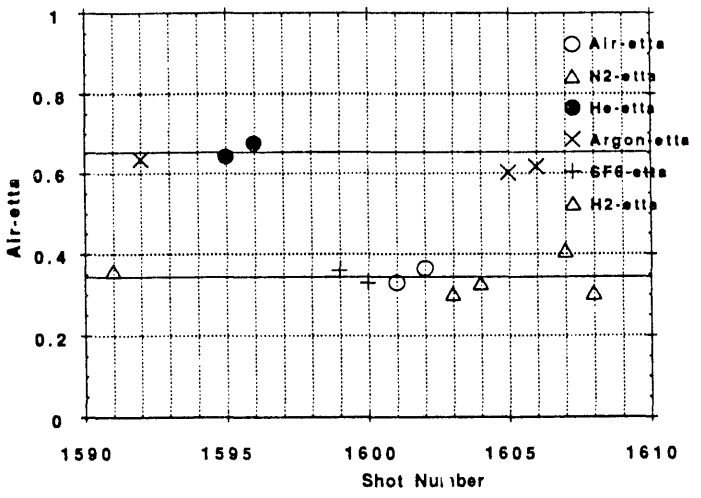

Figure 3

We found another way to place energy into the gas calorimeter that used exploding wires. Most metallic wires show large specific resistance changes (typically one to two orders of magnitude) between room temperature and burst. We decided to use Nichrome wire connecting the two electrodes with the hope that its resistance change would be minimal. Nichrome uses 80% nickel and 20% chromium to obtain a low temperature coefficient. First, we measured the wire's resistance with an ohm-meter. Next, we placed this wire in the test gap, blew it up with an electrical pulse while measuring the voltage and current. We calculated the pulsed resistance using the data and found that a barely exploding wire's measured pulsed resistance is the same as the bench test resistance. We also found that a wire exploding early in the pulse has a resistance that is too large for this method. The increase in voltage across the wire was easily observable. We set the Marx voltage where the opening voltage pulse was barely observable at the time of almost zero current.

We measure and calculate the energy deposited in the wire four different ways. First, we multiply the measured resistance by the measured Cvrl current squared (I^2) and integrate to provide the energy deposition. This procedure requires no time shifting or voltage monitor data. Second, the computer program time shifts, multiplies, integrates V and I, and then subtracts the inductor's energy. Third, we monitor the change in gas pressure during the shot and, using Fig. 2, calculate the energy deposited in the gas. Fourth, as another cross check, the handbook energy value to burst a nickel wire is 6762 J/gm. The actual energy in the report was 5492 J/gm (average=6127 ± 650 J/gm)[4]. Our experimental average will be given later.

By using three different wire sizes we obtained a reasonable data base. The damping resistance in the Ripple circuit was 7.5 ohms that provided a highly damped wave as show in Fig. 4. Note that even though the current wave forms are similar when the optional damping resistor is used, the voltage traces are different and the deposited energy changes. Six data shots for each wire size in nitrogen showed a small but measurable effect evidently caused by the wire mass. Experiments in SF_6 and air gave exothermic reactions with considerably more energy in the gas than calculated. Validyne Model AP10 pressure transducers provided the pressure measurements.

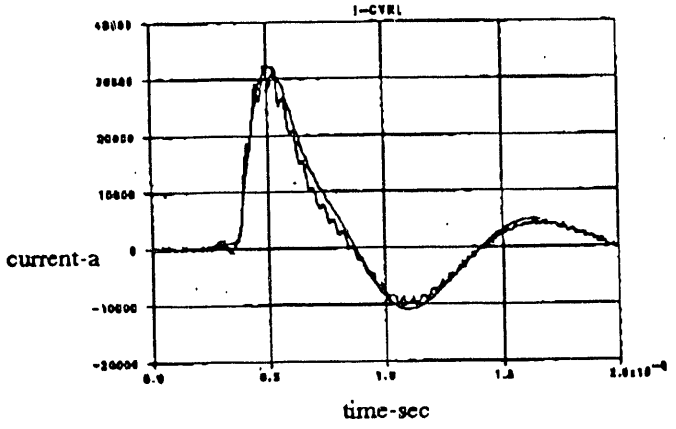

Figure 4

By extrapolating the measured gas energy divided by the measured electrical energy back to zero wire size, we find that the calorimeter measurement is within 9% of the recorded electrical energy. Figure 5 shows this data. The integrated I^2 R was essentially the same as the integral of V I. We found the average energy to burst the wire to be 6175 J/gm that is within 1% of the average value for nickel given above. Thus within reasonable error the experimental set up provides the correct energy dissipation in the test switch.

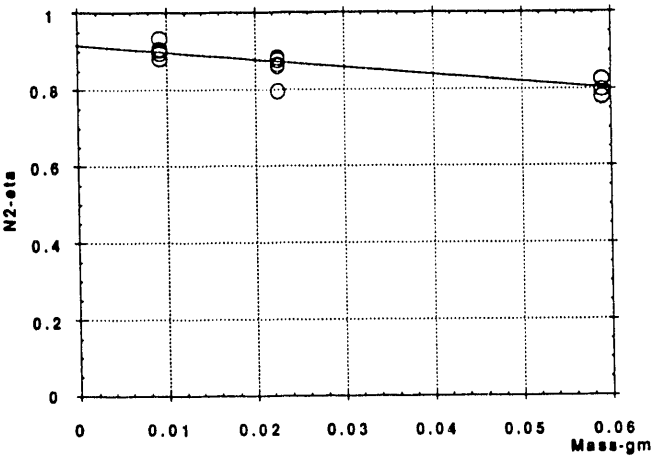

Figure 5

Experimental Results

The experiments used a variety of electrode types, dielectric types, and damping resistances. Electrode types were ball-ball, ball-plane, needle-plane, and rod-plane. Remarkably the electrode type did not make a difference in the energy dissipated except by causing a change in the gap distance. As will be shown, the energy loss is independent of the switching dielectric when viewed using the appropriate parameters.

The measured switch energy loss is one parameter. Two other obvious measured parameters are the peak voltage (V_{peak}) before switch breakdown and the peak switch current (I_{peak}) after switch breakdown. Multiplying these together provided a reasonable data grouping. We defined the energy loss in the switch as the energy lost at the end of the first current half cycle. This definition is adequate for capacitor to capacitor energy transfers. The capacitor to inductor

transfer requires a modification of the energy data. The energy loss at current peak is about 2/3 of the graph value for the 1/2 cycle energy.

Figure 6 presents the water data. Where possible, the plots include data from other experimenters. The open circles show the data points. The solid dots show the projected energy loss predicted by τ_r. Note that the dots are about a factor of 5 lower than the actual data. The data seems to have a tighter grouping on this plot than the τ_r prediction and at certain locations on the graph there is some overlap. The energy loss was determined by integrating the product of V and I with time and subtracting the inductive energy determined at the same instant.

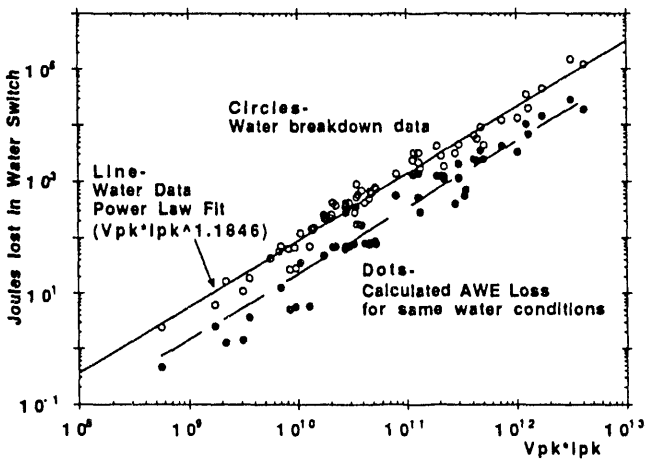

Figure 6

Although the data lies in a straight line on log-log plots, it is not a one to one slope. The energy dissipated in the switch is proportional to $(V_{peak}\ I_{peak})^n$ where n = 1.1846 ± .1. This exponent will provide a check on the theory later.

The data scatter indicates that the loss process involves other variables than V_{peak} and I_{peak}. However, defining the relationship between switch energy loss and V_{peak} and I_{peak} appears to be a first-principle condition.

Figure 7 shows the air test results. For comparison purposes the water power-law fit approximates the air data. The dots show the τ_r calculations. The τ_r predictions are approximately an order of magnitude away from the data.

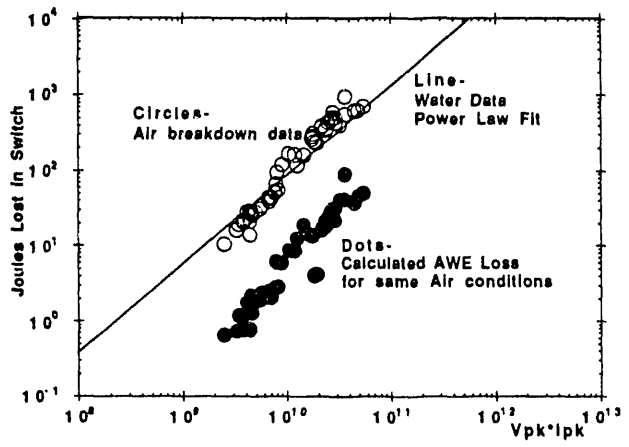

Figure 7

Figure 8 shows the SF6 data and the water data line. We notice again that the slope and separation from the τ_f predictions are considerable.

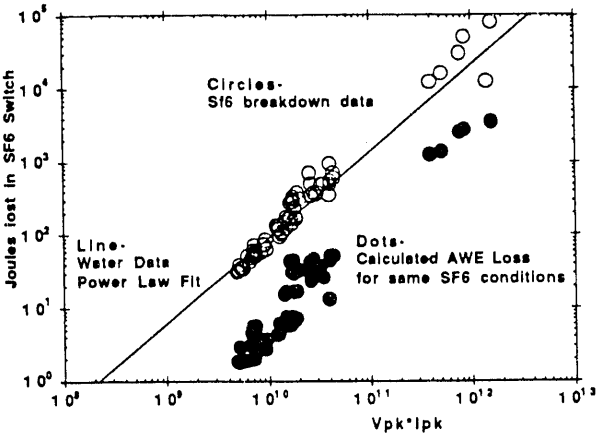

Figure 8

Figure 9 and Fig. 10 show helium and hydrogen. Stray capacity causes a pronounced droop in this data.

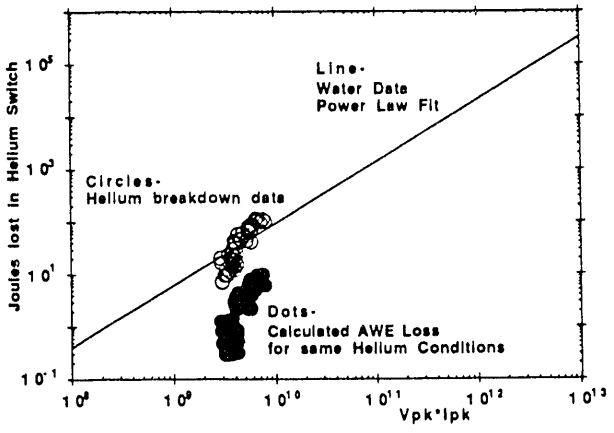

Figure 9

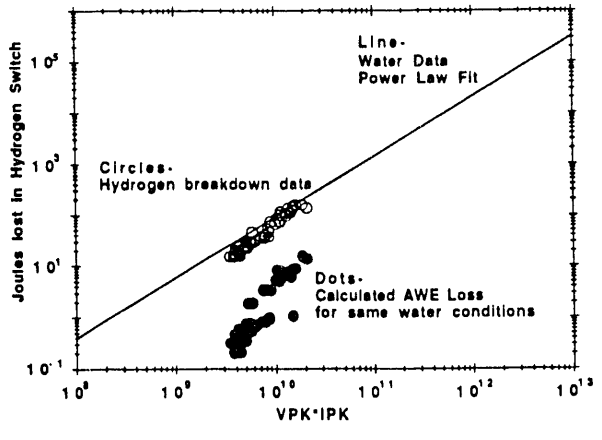

Figure 10

The consistency of the loss slope between the tested dielectrics indicates that similar phenomena were occurring in the spark channels of most media. We hoped that one theory is applicable to most dielectrics. The theory question is simplified because of the similarity. Is there a theory of breakdown that explains any single dielectric? If so, then that theory is applicable to our switching energy loss problem and leads to the next section on theory development.

The Theory Development Sequence

Considerable literature was available and published using lower energies, currents, and voltages. Most data concerned hydrogen or air as the working dielectric. The first hypothesis we tested was that nothing special seems to happen at τ_γ. The most convincing data found was by Martinen and Tholl.[5] A 20.4-nf capacitor drove a 2-cm gap with 460 Torr of hydrogen. The circuit inductance was 700 nh and was in series with a 1-ohm damping resistor. Tholl measured a peak channel current of 2200 amps along with the channel radius as a function of time. Figure 11 shows the combined plot of their experiment. The channel radius grows in a smooth and continuous manner while the current smoothly oscillates and decreases to zero. The time to peak current is 188 ns. The calculated τ_γ for this switch is 9.2 ns. If the channel requires energy to expand, then it requires energy much longer than the first 9 ns.

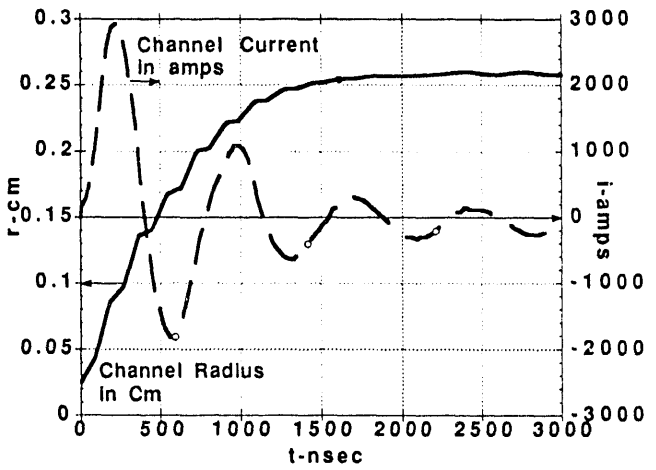

Figure 11

The next step in developing a theory is a recurring hypothesis of a constant conductivity plasma. If true, then the plasma calculations are greatly simplified. The constant conductivity plasma hypothesis was checked and will be presented.

Andreev and Orlov made a convincing case for constant plasma conductivity with data from a .84 cm atmospheric air gap.[6] Figure 12 shows the results. Their ringing discharge used a 5.5-nf capacitor charged to 20 kV which was switched into a 17.5-nh inductor. The calculated time to peak current was 9.8 ns while the actual time to peak current was about 20 ns. The authors measured the radius of the spark channel as a function of time and they wanted to see if a constant plasma conductivity would allow fitting of the current data. A true switch with infinite conductivity gives the sinusoid as shown. Andreev and Orlov assumed three other finite conductivities and calculated the currents. The 300 mho/cm conductivity fits the data closely. We recognized the familiar initial slowly rising current pulse generally attributed to the resistive rise time of 22.8 ns.

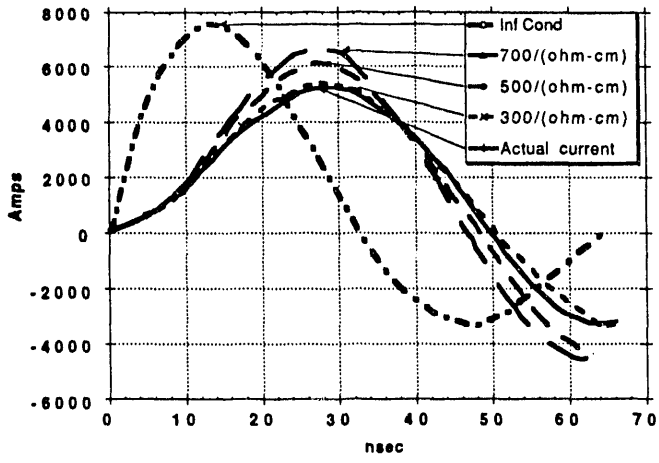

Figure 12

We can now hypothesize a basis for switching loss theory if the channel radius is predictable. Koppitz[7] did an important comparison between channel radius theory and experiments.

Koppitz made measurements on a 460 Torr air gap and compared the measurements with theory proposed by Braginskii[1] as shown in Fig. 13. Koppitz used a 10-nf capacitor ringing into a 840-nh inductor with a series damping resistor of 2.8 ohms. The Bragininskii Theory predicted the spark channel radius to 1.5 full cycles with a time to peak current of 144 ns. Thus the Braginskii Theory provides the spark channel diameter as a function of time.

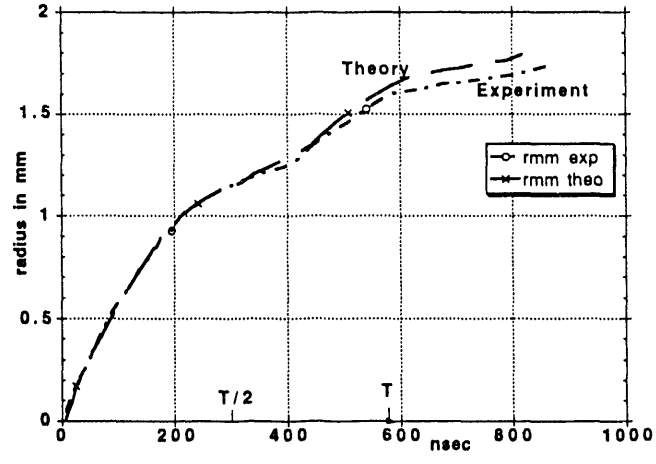

Figure 13

Braginiskii provides the final part of the theory. His article provides the spark channel phenomena. With some simplifying assumptions he solved the equations of the channel radius explicitly. Braginskii provided solutions for the gas motion inside and outside the channel by considering a shock wave. He then predicted the characteristics of the channel such as radius, temperature and pressure.

We quote from Braginiskii: "A comparatively narrow current-carrying channel is formed in the gas, with high temperature and ionization. Joule heat is released in the channel, which leads to an increase in the pressure and a thickening of the channel. The thickened channel acts like a piston on the remaining gas and, since the expansion takes place with supersonic speed, it produces a shock in the gas; this

shock is propagated in front of the original piston. The temperature in the vicinity of the shock is much higher than the gas at rest, and the temperature in the channel itself is still many times higher than the shock. Consequently, the density of the gas in the channel is very low, and the boundary of the channel acts as a piston."

Braginskii's equation 4.4 provides a good summary[1] and is given as equation 4. Braginskii solved this differential equation and found the power balance of the system.

$$\frac{I^2}{\sigma} = \rho_o 2\pi^2 a^3 \frac{da}{dt}^3 \xi \qquad (4)$$

where

$$\xi = K_p \left[1 + \frac{(2 - \frac{1}{k})}{(\gamma - 1)}\right] \qquad (4a)$$

K_p= .9 (coefficient of resistance constant)
γ= Cp/Cv the ratio of specific heat ≡ 1.4
k≡3/4 (an integration constant, also see below)

Note that ξ can be set to a constant value of about

$\xi \equiv 4.5$ for hydrogen
a= the channel radius
I= current

The general solution of this equation is

$$a \equiv A\, t^k$$

Braginskii assumed that

1. The removal of heat is through transparent radiation.
2. The thermal conductivity can be neglected.

Then

1. The pressure, temperature and density are constant over the cross section of the channel.
2. The entire temperature drop is in a thin shell where the radiation is absorbed.
3. The gas ionization takes place only in the shell.

Equation 4 can be solved for $a\frac{da}{dt}$

$$a\frac{da}{dt} = \frac{I^{2/3}}{(2\pi^2 \rho_o \xi \sigma)^{1/3}} \qquad (5)$$

and integrated by noting that $\frac{d(a^2)}{dt} = 2a\frac{da}{dt}$.

$$a^2 = \left[\frac{4}{\pi^2 \rho_o \xi \sigma}\right]^{1/3} \int_0^t I^{2/3}\, dt \qquad (6)$$

Since we need a^2 to calculate the channel resistance, this form is acceptable. Note that these formulas 4 through 6 are in the cgs system of units as used in the Braginskii article. Next the resistance of the channel is calculated.

$$R_{chan} = \frac{L_{cm}}{\sigma \pi a^2} \tag{7}$$

and this constitutes the theory needed to predict switching losses. Implementing into a circuit code program will be discussed next.

The Fortran Switching Energy Program

The computer program to calculate the energy dissipated in a breakdown can be based on equations 6 and 7. The circuit code SCREAMER is interactive and the switch breakdown resistance is fed back into the circuit.[8] Thus the switch and the circuit are interactive.

We wrote a Fortran program for the Screamer circuit code and then computed the electrical parameters as a function of time for all of the data. A constant was determined from equation 6 which we called the Braginskii constant. Note that these units are in cgs and must be converted. to the appropriate units before use.

$$C_{Brag} = \frac{4}{\pi^2 \rho_o \xi \sigma} \tag{8}$$

$\xi = 4.5$ for hydrogen was determined from the Braginskii paper and then used for all media. A closer approximation could have been obtained if channel radius data were available. The densities in gm/cc are handbook values. The conductivity was obtained from Andreev and Orlov for air then modified to obtain the best fit with our data. This modification also compensated for not allowing ξ to change. Table I provides the values used in our simulations. Note that oil, although included in the table for future use, was not tested during our experiments.

Table I

Material	Conductivity in mho-cm	ρ_o in gm/cc at 14.7 psia	$\frac{\rho_o^{1/3}}{\sigma^{2/3}}$
H_2O	600	1.0	.0141
Oil	600	.9	.0135
SF_6	160	$6.160*10^{-3}$	.00622
Air	200	$1.293*10^{-3}$	.00319
Helium	140	$1.780*10^{-4}$	.00209
Hydrogen	300	$8.990*10^{-5}$	.00100

Comparison of Theory and Experiment

Switch Loss Energy and V_{peak} I_{peak} Scaling is Explained

We can obtain interesting insights and solve the above equations if I is allowed to be a linear function of t.

$$I_1(t) = K_1 t \tag{8a}$$

$$a2 = \left[\frac{4}{\pi^2 \rho_o \xi \sigma}\right]^{1/3} K_1^{2/3} \int_0^t t^{2/3}\, dt \tag{8b}$$

integrating between 0 and t

$$a2 = C_{Brag}^{1/3} K_1^{2/3} \frac{3}{5} t^{5/3} \tag{8c}$$

$$Power_{channel} = Resistance_{channel}\, I_1^2 =$$

$$\frac{K_1^2 t^2 L_{cm}}{\sigma \pi C_{Brag}^{1/3} K_1^{2/3} \frac{3}{5} t^{5/3}}$$

$$\frac{5 K_1^{4/3} t^{1/3} L_{cm}}{3 \sigma \pi C_{Brag}^{1/3}} \qquad (8d)$$

The switch channel energy $Energy_{channel}$ is the integral of $Power_{channel}$ or

$$Energy_{channel} = \frac{5 L_{cm}}{3 \sigma \pi C_{Brag}^{1/3}} \int_0^t K_1^{4/3} t^{1/3} dt =$$

using 8a)

$$\frac{5 L_{cm} 3}{3 \sigma \pi C_{Brag}^{1/3} 4} K_1^{4/3} t^{4/3} =$$

$$\frac{5 L_{cm} I_1^{4/3}}{4 \sigma \pi C_{Brag}^{1/3}} \qquad (8e)$$

Note that the current rise rate is absorbed in the $I^{4/3}$ and the energy deposited in the channel is dependent on peak current and not time. Equation 8e is a true scaling equation and will cross check our data sets. In most of our testing the voltage V_{peak} is proportional to the length (L_{cm}). Allowing I_1 to be I_{peak} and noting that $V_{peak} \alpha I_{peak}$. The energy relationship provides the following:

$$Energy_{channel} \alpha \frac{5 V_{peak} I_{peak}^{4/3}}{4 \sigma \pi C_{Brag}^{1/3}} \alpha$$

$$\frac{5 [V_{peak} I_{peak}]^{7/6}}{4 \sigma \pi C_{Brag}^{1/3}} \alpha \rho_0^{1/3} [V_{peak} I_{peak}]^{1.167} \qquad (8f)$$

The exponent of 1.167 in 8f compares to the value of 1.1846 ± .1 that was obtained from the best fit power curve on the water data as shown above. Deriving essentially the same exponent for the switch loss scaling between the data and theory gives confidence that we are describing and observing the same basic phenomena.

Explaining the Marx Switch Series Resistance Paradox

Marx generators consist of many series connected switches and capacitors to form high voltage outputs. Because of their high inductances and stored energy, the main energy is transferred long after τ_r. The τ_r method of energy prediction indicates little switch loss. However, we have needed an unexplained series resistance which dissipates appreciable energy to get the circuit simulation to agree with the actual output. Previously the source of this resistance was not clear but fortunately the value of this resistance has decreased as the Marx energy increased. The result is that the efficiency of the Marxes is about constant over a large number of designs. Simple scaling extrapolations failed. Scaling estimates were sometimes based on the average resistance per spark gap. Alternatively, attempts to measure this resistance

by short circuit shots and ringing shots which gave different values for this unexplained resistance.

When we replaced this constant series resistance with the new model then the theory and data agreed over several cycles. Now the Marx resistance is modeled by allowing the switch length d to be the number of gaps multiplied times each gap's length. We can now predict the Marx generator's series loss. The model predicts a loss that depends on the peak current and explains why the apparent resistance changes between short circuit and open circuit tests. The model explains why the Marx efficiency has remained relatively constant.

The Data and Experiment Agree

Using the model we now can predict using additional variables other than V_{peak} I_{peak}. For instance, we did not apply any correction for varying the gap pressure or for the switch breaking at the appropriate phase angle of the charging pulse. Another important variable is the stray capacity across the gap. When we used gas, the gap housing was immersed in water and the stray capacity energy was about equal to the gap energy on the low energy shots. With the added analysis capability, we needed a new method for comparing the data and theory.

The comparison method chosen calculates the peak current and the energy loss in the gap during the first current half-cycle. We plotted all of the dielectrics on the same graph to show the similarity between the various dielectrics. Figure 14 shows the experimental and theoretical energy losses. The estimated experimental error of ±30% is consistent with the data scatter. Within experimental error, the experiment and theory energy losses agree.

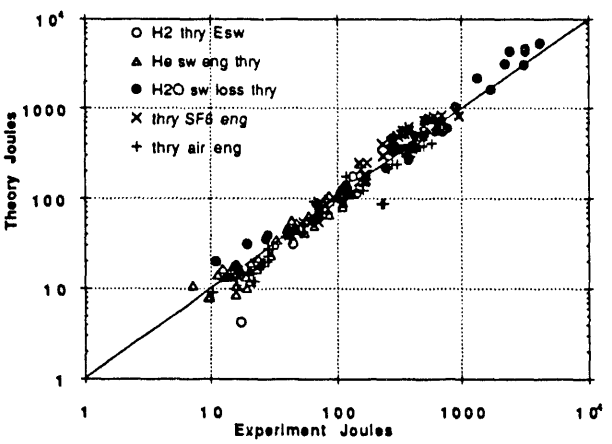

Figure 14

We converted the peak currents, both measured and calculated to $(I_{peak})^{4/3}$ d $(\rho/\rho o)^{1/3}$ and plotted the current results in Fig. 15 for water. We estimated the error bars in the current measurement at ±10%. The current measurement theory also has error bars estimated at ±10% because we used the measured voltage peak to determine the switch closure time. The smaller expected errors are consistent with this comparison and better agreement is obtained between experiment and theory. The peak currents appear predictable using this model.

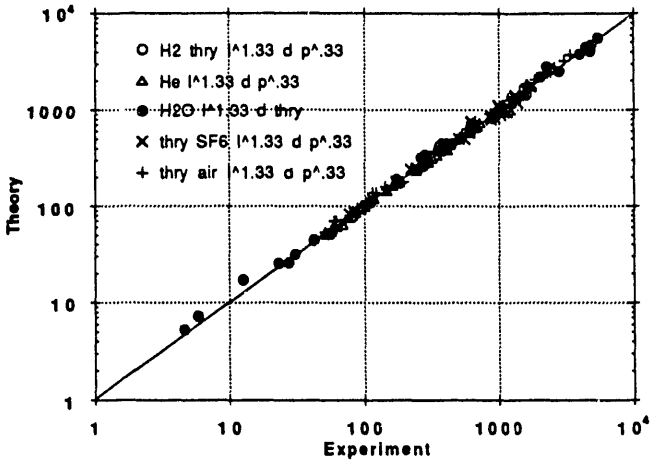

Figure 15

For comparison during subsequent cycles Fig. 4, already presented, shows the predicted and actual currents for a damped ring down discharge where only a few cycles are present. Figure 16 shows the theory and experiment comparison for a ringing discharge. The Ripple experiment consisted of a 1-cm air gap between a 2-inch diameter hemisphere and a ground plane operating at 90 psia with no damping resistor. Note that the simulation uses the same model for the Marx series resistance and that this comparison really has two gaps operating in series to provide this solution.

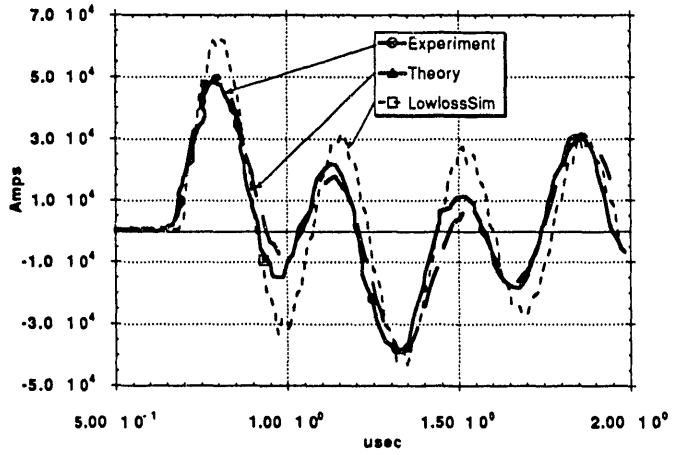

Figure 16

In an effort to compare the model predictions with a loss-less model, the low loss simulation is shown in Figure 16. The Marx generator loss was modeled by substituting a constant resistance to provide the correct ringing gain and then the current was found for a loss-less switch. The first peak current is about 25% higher than either measured or calculated for this particular case and the switch causes a significant loss of energy into an inductive energy store.

Stray Capacity, Another Comment on the Model

The effect of stray capacity is important for special application switches. As determined from our computer solutions, the stray capacity under certain conditions can supply the fastest available

energy to heat the breakdown channel. If the stray capacity energy is an appreciable then the switch losses and rise times are modified. For an example of this simulation being applied to a 100-ps rise switch see Ref. 9.

Summary

A useful method and theory providing switching loss estimates were presented. The method appears to be correct as shown by comparison between theory and experiment. The losses are significant and considerably larger than previously predicted.

Acknowledgments

We would like to thank D. R. Humphreys for his early work on the spark breakdown process, for his continuing technical discussions, and for his review and comments on this article. We thank K. S. Ward for operating the instrumentation room, taking our data, and having more understanding than we deserved during our calibration runs.

Finally, we recognize again the early work done by J. C. Martin and his associates at the Atomic Weapons Establishment on the spark breakdown and energy loss estimations. We remember the first comments you gave, "use with caution and check it out." We can only hope that this article's contribution to estimating switching loss will approach the usefulness of yours at AWE.

References

[1] S. I. Braginskii, "Theory of the Development of a Spark Channel," *JETP*, Vol. 34 (7), No. 6, p. 1068, December 1958.

[2] J. C. Martin, "Duration of the Resistive Phase and Inductance of Spark Channels," SSWA/JCM/1065/25 Atomic Weapons Research Establishment Paper.

[3] A. Mandl and E. Salesky, "Electron Beam Deposition Studies of the Rare Gases,"*J. Appl. Phys.*, Vol 60, No. 5, **1** Sept. 1, 1986.

[4] T. J. Tucker and R. P.Toth, "EBW1: A Computer Code for the Prediction of the Behavior of Electrical Circuits Containing Exploding Wire Elements," SAND-75-0041, Sandia National Laboratories Report, Albuquerque , NM , 87185.

[5] H. Martinen and H. Tholl, "Investigation of the Temperature and Expansion the Spark Channel in H_2 with Variable Energy Inputs," Z. Naturforsch. 25A, 1970, p 430

[6] S. I. Andreev and B. I. Orlov, "Development of a Spark Discharge. I," Soviet Physics-Technical Physics, Vol 10, No. 8, Feb., 1966. p. 1097.

[7] J. Koppitz, "The Radial and Axial Development of a Spark Channel Recorded with a Streak Camera," Z. Naturforsch, 1969, 22A, p. 1089.

[8] M. L. Kiefer, K. L. Fugelso, and M. M. Widner, "SCREAMER: A Pulsed Power Design Tool," Sandia National Laboratories Internal Report, June 26, 1991.

[9] A. Frost, P. E. Patterson, L. D. Roose, L.F. Rinehart, T. H. Martin, "Picosecond High Pressure Gas Switch Experiment," 1993 Pulsed Power Conference Proceedings, Albuquerque, NM.

---

*This research was supported by the U. S. Department of Energy under contract DE-AC04-76DP00789.

†Ktech Corp., Albuquerque, NM 87110

DATE
FILMED
9/10/93
END